Polymer Chemistry

PAPER

Check for updates

Polymers from sugars and CO_2: ring-opening polymerisation and copolymerisation of cyclic carbonates derived from 2-deoxy-D-ribose†

Georgina L. Gregory, [a,b] Gabriele Kociok-Köhn [c] and Antoine Buchard*[a]

Bio-based aliphatic polycarbonates (APCs) are attractive synthetic materials for biomedical applications because of their biodegradabilty and biocompatability properties. A high yielding 3-step process that utilises CO_2 as a C1 synthon is presented for converting raw sugar, 2-deoxy-D-ribose into a novel 6-membered cyclic carbonate for ring-opening polymerisation (ROP) into carbohydrate-based APCs. The α- and β-anomers of the monomer could be isolated and revealed very different polymerisability, as rationalised by DFT calculations. Whereas the β-anomer could not be polymerised under the conditions tested, organocatalytic homopolymerisation of the α-anomer, in solution at room temperature (rt) or under melt conditions, yielded highly insoluble polycarbonates, composed of both cyclic and linear topologies, and exhibiting a glass transition temperature (T_g) of ~58 °C. Random copolymers with controllable incorporation of this new sugar monomer were prepared with trimethylene carbonate (TMC) at rt in the bulk or in solution with M_n up to 64 000 g mol^{-1}. With increasing sugar content, the T_g values of the copolymers increased and their thermal degradability was enhanced, giving access to a new class of APCs with tailored properties.

Introduction

The design of new synthetic polymers which draw upon renewable resources is important both for alleviating our reliance on dwindling fossil-based feedstocks and for the continued generation of materials with advanced properties.[1] In particular, biocompatibility and biodegradability are desired properties for polymer applications within the biomedical field and for mitigating the end-of-life environmental impact of plastics.[2] Natural monosaccharides are one renewable alternative to petroleum-based resources. They present a pool of readily available and functional building blocks that are cheap, stereochemically rich and non-toxic.[3] In addition, the rigid cyclic structure adopted by many sugars, when retained in a polymer

*a*Department of Chemistry, University of Bath, Claverton Down, Bath BA2 7AY, UK.
E-mail: a.buchard@bath.ac.uk; Fax: +44 (0)1225 386231; Tel: +44 (0)1225 386122
*b*Centre for Doctoral Training in Sustainable Chemical Technologies, University of Bath, Bath BA2 7AY, UK
*c*Chemical Characterisation and Analysis Facility (CCAF), University of Bath, UK
†Electronic supplementary information (ESI) available: NMR spectra of monomer and polymers. Single-crystal X-ray diffraction data for **1α** and **1β**. Plot of M_n and *Đ* vs. conversion, calculation of reactivity ratios and copolymerisation kinetic data. Images of SEC traces, TGA-MS, MALDI-ToF MS, DSC traces and powder diffraction data. DFT calculations data and associated digital repositories. CCDC 1532104 and 1532105. For ESI and crystallographic data in CIF or other electronic format see DOI: 10.1039/c7py00236j

backbone, can result in enhanced material properties such as high glass transition temperatures (T_g).[4] Synthetic carbohydrate-based polymers can also serve as functional analogues of biomacromolecules, the high hydroxyl group content providing huge scope for functionalisation and modification of polymer properties.[3a,5]

With regard to classes of polymers, the construction of bio-based aliphatic polycarbonates (APCs) and polyesters such as poly(lactic-*co*-glycolic acid) (PLGA) have received much attention as biodegradable materials for use in tissue engineering scaffolds and drug delivery systems.[1c,6] Non-acidic degradation products, reducing potential adverse side reactions, and typically slower degradation rates of carbonate units, prolonging the lifetime, have further driven interest in APCs and their copolymers for *in vivo* applications.[2,7]

APCs are typically prepared by three alternative routes, with firstly, the polycondensation of aliphatic diols with phosgene, phosgene derivatives or dialkyl carbonates.[8] Polycarbonates of isosorbide[9] and functionalised D-glucose sugar diols[10] have thus been prepared this way. Although industrially used, this step-growth polymerisation can present drawbacks in terms of high temperatures, long reaction times, poor chain length control and limited access to copolymers. Secondly, motivated by the direct utilisation of CO_2 as a safe, abundant and renewable feedstock, extensive developments have been made in catalysis for APC synthesis by the ring-opening copolymerisation (ROCOP) of

epoxides with CO_2.[11] This approach however can be limited by molecular weight control, as well as catalyst and substrate scope, in particular with sugar resources. Finally, driven by the release of ring-strain, the ring-opening polymerisation (ROP) of cyclic carbonate monomers is an attractive method for achieving high molar mass and well-defined polycarbonates.[12] In addition to the many metal-based catalysts,[13] a variety of simple organocatalytic systems including 4-dimethylaminopyridine (DMAP), 1,8-diazabicyclo[5.4.0]undec-7-ene (DBU), 1,5,7-triazabicyclo[4.4.0]dec-5-ene (TBD), 4-pyrrolidinopyridine (PPY), ureas,[14] thioureas (TU),[15] N-heterocyclic carbenes as well as various phosphines, phosphazenes[16] and organic phosphoric acids[17] have been shown to promote ROP under mild and metal-free reaction conditions.[18] Typically, cyclic carbonates for ROP are 6-membered rings though there are examples of 7-,[19] 8-[20] and highly strained 5-[21] membered ring monomers. The usually low ring strain of 5-membered cyclic carbonates often means that forcing ROP conditions are required, which result in decarboxylation and ether linkages in the polymer backbone, detrimental to its physical properties. Preparation of cyclic carbonate monomers commonly involves the transesterification of diols with phosgene derivatives, and although recent advances have been made, including using CO_2,[22] improvements are still required to limit the use of stoichiometric reagents.

In parallel, a growing research trend has focused on the synthesis of 6-membered cyclic carbonates from bio-sourced diols.[23] Although advantageous for introducing functionalities and modifying polymer properties (such as solubility and hydrolytic degradation rate), the high hydroxyl group content of sugars often entails the use of protecting group chemistry to avoid undesired reactions during ROP.[3b] To date, sugar-based cyclic carbonate monomers include those derived from D-mannose,[24] D-glucose[25] and D-xylose.[26] 2-deoxy-D-ribose is a readily available and simple pentose sugar, which lack of utility in APC synthesis by ROP so far can be attributed to its thermodynamically favoured 6-membered pyranose ring form. This indeed exposes a *cis*-1,2-diol, the cyclocarbonation of which yields a low ring-strained 5-membered cyclic carbonate (Fig. 1). In contrast with the 5-membered cyclic carbonate *trans*-fused to the pyranose ring of glucose reported by Endo,[27] Tezuka *et al.* showed that the analogous *cis*-fused monomers

do not readily undergo ROP.[28] However, 2-deoxy-D-ribose in its furanose form, in which it composes the core of DNA, consists of a *trans*-1,3-diol providing access to a desired 6-membered cyclic carbonate. Nevertheless, cyclocarbonation of this motif, although attempted, has never been isolated. This is postulated to be due to its highly strained and thus unstable nature.[29]

Thus, we set out to prepare a *cis*-6-membered cyclic carbonate of 2-deoxy-D-ribofuranose for ROP under mild reaction conditions, using our recently developed method of CO_2-driven cyclocarbonation with stereochemical inversion.[30] We hoped that the chirality of the anomeric carbon coupled to the rigid furanose ring would also impart interesting properties to the polymer backbone, both in the homopolymers and in copolymers with other monomers. Indeed, the ability to tailor polymer properties such as degradation rates and T_g through copolymerisation is important for designing polymers with wider potential applications. For example, poly(trimethylene carbonate) (PTMC) prepared by the ROP of trimethylene carbonate (TMC) is a flexible, hydrophobic and non-crystalline plastic exhibiting a T_g of around -20–-30 °C.[27,31,33] The fine-tuning of these properties have been extensively studied[32] with well-known examples including copolymers of TMC with lactide,[33] glycolide[34] and caprolactone.[35] In our case, the cyclic structure of carbohydrate-based monomers would be well placed to impart stiffness to polymer chains.[36]

Herein, we report the synthesis of novel α- and β-cyclic carbonate monomers from raw carbohydrate 2-deoxy-D-ribose and CO_2 C1 synthon, their organocatalytic ROP and the thermal properties of the resulting new polycarbonates. We also used DFT calculations to rationalise the differences observed in the polymerisability of the α- and β-anomers. Copolymerisation with TMC was finally studied, providing high molecular weight random APC copolymers with controlled sugar monomer content and designable thermal properties.

Results and discussion

Monomer synthesis

Monomer **1** (Scheme 1) was prepared as a 50 : 50 mixture of α- and β-anomers in three high yielding steps from natural sugar,
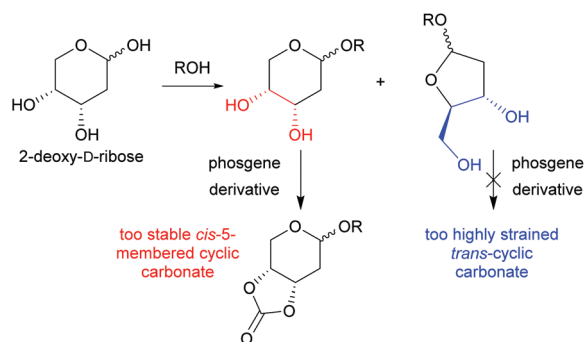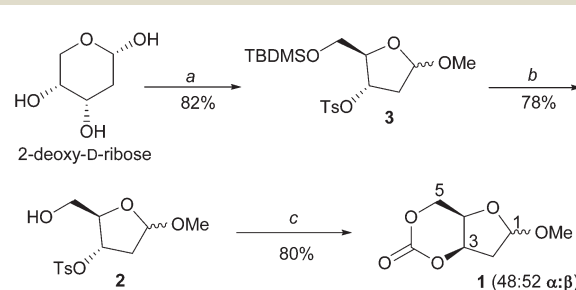

Fig. 1 Challenges in the synthesis of cyclic carbonate monomers from 2-deoxy-D-ribose.

Scheme 1 Synthesis of 6-membered *cis*-cyclic carbonate **1** from 2-deoxy-D-ribose: a: (i) MeOH, HCl, 0.5 h (ii) TBDMSCl, pyridine, cat. DMAP, 2 h (iii) TsCl, 12 h; b: 1 wt% I_2 in MeOH, reflux, 4 h; c: DBU, CO_2, MeCN, 0° to rt, 24 h.

2-deoxy-D-ribose. Following kinetic trapping of the sugar ring in its 5-membered furanose form by methylation of the anomeric hydroxyl group, sequential silyl protection of the 5-position and tosylation of the 3-position was carried out in the same reaction pot. Deprotection of the silyl group was achieved under mild reactions conditions with I_2 in MeOH and CO_2 inserted (at 1 atm pressure) using DBU reagent into the now exposed primary hydroxyl group. *In situ* cyclisation of the resulting carbonate nucleophile proceeded at room temperature (rt) *via* an intramolecular S_N2-type displacement of the tosyl group resulting in inversion of the stereochemistry at the 3-position.

The α- and β-anomers of the subsequently *cis*-configured 6-membered cyclic carbonates were furthermore separated by column chromatography and recrystallisation from dry ether and toluene, respectively. The use of CO_2 here is vital for obtaining these monomers from D-ribofuranose sugar, as phosgene derivatives only promote a nucleophilic addition–elimination pathway. Both **1α** and **1β** were fully characterised by elemental analysis, NMR (Fig. S1–S10 in the ESI†) and FT-IR spectroscopies, electrospray ionisation mass spectrometry (ESI-MS) and single-crystal X-ray diffraction. *J*-Coupling constants ($^3J_{34}$) in the ^1H NMR spectra of 4.9 and 5.7 Hz for the α- and β-anomers, respectively were consistent with *cis*-configured cyclic carbonates. This was further confirmed by single crystal X-ray diffraction of crystals grown by layering hexanes over chloroform. The furanose ring in **1β** adopts a 2-*exo* (E_2) envelope conformation whereby C5 puckers below the plane formed by C4–C3–O4–C6 (dihedral angle ∼2°) (Fig. 2 right). In contrast, the α-anomer adopts a more twisted conformation ($^0T_1/E_1$), with C6 below and O4 above the plane formed by C5–C4–C3 (Fig. 2 left). This difference in conformation of the ribofuranose ring later proved to have a marked impact on the ring strain and thus ROP reactivity of the fused cyclic carbonate.
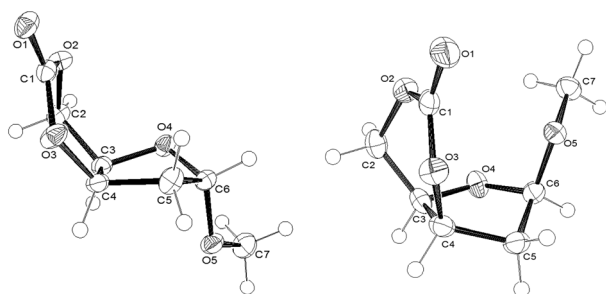
Ring-opening polymerisation

The homopolymerisation of **1α** was carried out with benzyl alcohol initiator and widely used bifunctional organocatalyst, TBD.[37] Over a range of initial monomer concentrations ($[M]_0$ = 1–5 mol L^{-1}), catalyst loadings (0.1–2 mol%) and monomer-to-initiator feed ratios ($[M]_0/[I]_0$ = 50–1000), a polymer invariably precipitated from solution during the reaction and was found to be highly insoluble in all common organic solvents as well as water, DMF and DMF/LiBr. Solubility in hexafluoroisopropanol (HFIP) however, enabled estimation of the number average molecular weight (M_n) and polymer dispersity (Đ) by size-exclusion chromatography (SEC). For a polymerisation with $[M]_0$ of 5 mol L^{-1} in CH_2Cl_2, $[M]_0/[I]_0$ of 400 and 0.25 mol% catalyst loading, the polymer precipitated after 1 h and had an M_n of 25 600 g mol^{-1} (Đ 1.41) relative to PMMA standards.

MALDI-ToF MS analysis revealed a mixture (∼1:1) of both linear and cyclic polycarbonate species but of much lower M_n (Fig. 3 and S29†). This may be due to PMMA being a poor standard for the ribose-based polycarbonates or difficulties in ionising higher M_n species during the MALDI process. NMR and SEC analysis of the supernatant revealed unreacted monomer and lower M_n oligomers. At this initial monomer concentration of 5 mol L^{-1}, monomer conversion could be monitored before polymer precipitation, by integration of the ^1H NMR spectrum in $CDCl_3$ of aliquots taken and quenched with benzoic acid. A plateau was reached at 60% conversion (Fig. S20†). Further addition of monomer led to the establishment of a new equilibrium monomer conversion indicating no catalyst deactivation and a concentration dependent equilibrium polymerisation. A lower monomer conversion of 42% was achieved at a lower $[M]_0$ of 1 mol L^{-1}. Under melt conditions (T_m **1α** = 67–68 °C) with the same catalyst and initiator loadings (0.25 mol%), a limiting conversion of 51% was observed and an M_n of 22 300 g mol^{-1} (Đ 1.21) determined by SEC *versus* PMMA standards. The study of the temperature dependence of the ROP equilibrium and the reliable determi-
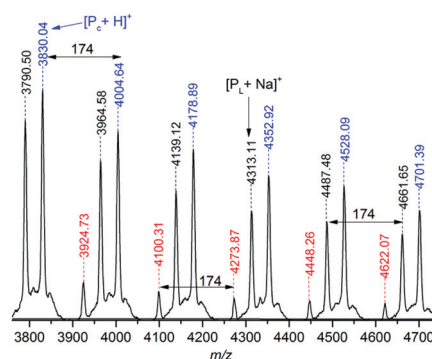

Fig. 2 ORTEP drawings with thermal ellipsoids at the 30% probability level for **1α** (left); selected bond lengths (Å) and torsion angles (°): C(1)–O(1) 1.1985(19), C(1)–O(2) 1.3325(19), C(1)–O(3) 1.342(2), O(4)–C(3)–C(4)–C(5) −9.34(15), C(3)–C(4)–C(5)–C(6) −14.60(15), C(4)–C(5)–C(6)–O(4) 34.21(15), C(5)–C(6)–O(4)–C(3) −41.74(15), C(4)–C(3)–O(4)–C(6) 31.81(15) and **1β** (right); selected bond lengths (Å) and torsion angles (°): C(1)–O(1) 1.1995(19), C(1)–O(2) 1.333(2), C(1)–O(3) 1.333(2), C(3)–O(4)–C(6)–C(5) 22.07(16), C(6)–O(4)–C(3)–C(4) −1.96(17), O(4)–C(3)–C(4)–C(5) −18.81(17), C(3)–C(4)–C(5)–C(6) 31.09(16), O(4)–C(6)–C(5)–C(4) −32.95(16).

Fig. 3 MALDI-ToF MS of poly(**1α**) in the region from 3750 to 4750 *m/z* showing cyclic polymeric series $[P_c + H]^+$ (*e.g.* DP = 26 gives *m/z* 4528.91) and linear polymer series with benzyl alcohol end-group, $[P_L + Na]^+$ (*e.g.* DP = 24 gives *m/z* 4310.73). The less intense red series may be assigned to the sodium adduct of the linear polymer with the loss of 1 CO_2.

nation of **1α** ROP thermodynamic parameters however, were prevented by the precipitation of the polymer from solution, especially at low temperatures.

Comparison of the ^{1}H NMR spectra of the monomer (Fig. 4A) to that of the polymer in HFIP-d$_2$ (Fig. 4B) showed a characteristic broadening of the proton signals alongside a coalescing of the ring methylene H-2 environments in the polymer. Estimation of the molecular weight by relative integration of these signals to those of the benzyl alcohol end-group gave a M_n much larger than that anticipated based on the monomer-to-initiator feed ratio and is consistent with the presence of cyclic species bearing no end-groups. The carbonate region of the ^{13}C{^{1}H} NMR spectrum (Fig. 4C) revealed three carbonate signals at 154.3, 154.0 and 153.6 ppm assigned to ring-opening at either side of the unsymmetrical monomer leading to tail–tail (TT), head–tail (HT) and head–head (HH) linkages, respectively. Quantitative ^{13}C{^{1}H} NMR spectroscopy revealed a roughly 1 : 2 : 1 ratio of these signals indicating a regiorandom polymer as also observed for reported D-glucose-[25] and D-xylose-[26] based polycarbonates.

In contrast, **1β** did not undergo homopolymerisation with organic bases (TBD, DBU and DBU/TU combination) or metal-based catalysts: Al(OTf)$_3$, Y(^{t}OPr)$_3$ and Sn(Oct)$_2$ in CH$_2$Cl$_2$, toluene, dioxane and THF solvents over a temperature range of −78–120 °C as well as under melt conditions (mpt **1β** = 106–108 °C). With Al(OTf)$_3$ catalyst and BnOH initiator, mutarotation of **1β** to the equilibrium ratio of **1α** : **1β** was observed with no polymerisation. A 50 : 50 feed ratio of both anomers, as an eutectic oil or in CH$_2$Cl$_2$ (5 mol L^{-1}) led at rt to polymerisation of the α-anomer only with no evidence by NMR spectroscopy of incorporation of **1β**.
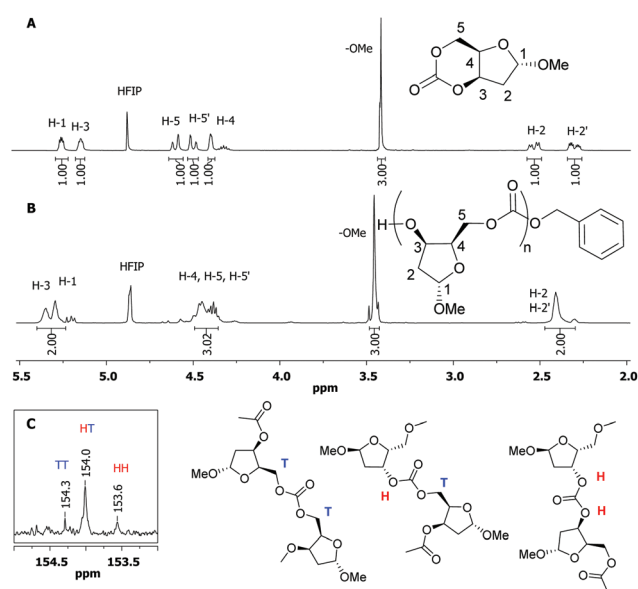
DFT modelling of the ROP initiation step provided an insight into the different behaviour of the two anomers (Fig. 5 and S36†). As seen previously,[24] ring-opening was found to be a 2-step process, with TBD mediating proton transfer through tetrahedral intermediates. The lowest limiting kinetic barriers ($\Delta\Delta G^{\ddagger}$) calculated for **1α** and **1β** opening were +10.0 and +13.8 kcal mol^{-1} respectively, low enough for both reactions to happen at rt. For comparison, $\Delta\Delta G^{\ddagger}$ for TMC initiation was +14.1 kcal mol^{-1} at the same level of theory. The overall thermodynamics of ring-opening presented however significant differences. Whereas ring-opening of TMC and (to either side) of unsymmetrical **1α** was favoured ($\Delta\Delta G$ = −0.9 to −1.9 kcal mol^{-1}), ring-opening of **1β** was calculated to be unfavourable ($\Delta\Delta G$ = +1.4/+2.0 kcal mol^{-1} to expose a primary or secondary alcohol group for chain propagation, respectively). In the ROP of **1β**, the equilibrium must lie well over to the monomer. In accordance with the experimentally observed random cleavage at either side of the carbonate in **1α**, little preference was found for opening **1α** to either a primary or secondary growing alcohol chain.

The difference in ring strain of **1α**, **1β** and TMC was further evaluated by calculating the enthalpy of the isodesmic ring-opening reaction with dimethyl carbonate (DMC) and the thermodynamics of ring-opening with primary and secondary alcohols. Both support the more highly strained nature of **1α** compared to **1β** and reveal a similar ring strain for **1α** to that of TMC (Schemes S2 and S3†). For example, based on the
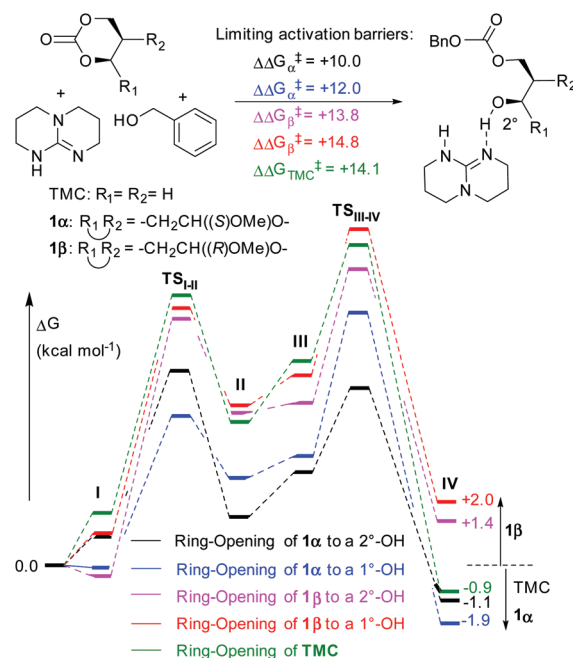

Fig. 4 Comparison of the ^{1}H NMR spectra (400 MHz, HFIP-d$_2$) of **1α** (A) and its homo-polymer (B). The carbonate region of the ^{13}C{^{1}H} NMR spectrum (400 MHz, HFIP-d$_2$) of the homopolymer (C) is also shown with assigned tail–tail (TT), head–tail (HT) and head–head (HH) regiochemistries.

Fig. 5 DFT modelling of the initiation step in the ROP of **1α**, **1β** and TMC with TBD catalyst and BnOH initiator involving formation of ternary complex I, nucleophilic addition of BnOH (TS$_{I−II}$) to form quaternary intermediate II, TBD migration III for ring-opening (TS$_{III−IV}$) to expose a primary (1°-OH) or secondary alcohol (2°-OH) in IV (see ESI† for full details, including structures and energies of all intermediates and TS).

isodesmic reaction, values of $\Delta\Delta H_{ring\ strain}$ of -6.6, -6.5 and -4.6 kcal mol^{-1} were calculated for $\mathbf{1\alpha}$, TMC and $\mathbf{1\beta}$, respectively.

Copolymerisation

For a 50 : 50 feed ratio of $\mathbf{1\alpha}$: TMC, the copolymerisation could be carried out in the absence of solvent at rt, with TBD organo-catalyst and benzyl alcohol initiator. A similar eutectic melt formation had also been observed on mixing L-lactide with TMC.[38] After 3 h with 0.1 mol% catalyst and $[M_t]_0/[I]_0$ of 1000, stirring was significantly perturbed because of the increased viscosity and the polymerisation quenched. NMR analysis showed, although incomplete, conversion of both monomers. Conversely to the homopolymerisation of $\mathbf{1\alpha}$, the product of the reaction was soluble in common organic solvents, and SEC analysis in CHCl$_3$ eluent *versus* polystyrene standards revealed a unique polymer distribution with a M_n of 64 000 g mol^{-1} (Table 1, entry 1), suggesting formation of a true copolymer rather than two separate homopolymers.

Monomer conversion was then monitored as a function of time for a polymerisation carried out at rt with the same catalyst and initiator loadings (0.1 mol%) but with an initial total monomer concentration ($[M_t]_0$) of 5 mol L^{-1} in CH$_2$Cl$_2$. This allowed aliquots to be taken, quenched and conversion evaluated by ^{1}H NMR spectroscopy (Fig. 6A). $\mathbf{1\alpha}$ was consumed faster compared to the TMC co-monomer, reaching 98% conversion after 10 h compared to 84% for TMC. Based on the near full conversion of $\mathbf{1\alpha}$, copolymerisation could overcome the thermodynamic limitation observed in the homopolymerisation of the sugar-derived monomer, suggesting a random or alternating copolymer.

Kinetic plots (Fig. 6B) showed pseudo first-order kinetics in monomer concentration, typical of ROP, from which k_{app} values of 0.262 ± 0.004 h^{-1} and 0.154 ± 0.002 h^{-1} were determined for $\mathbf{1\alpha}$ and TMC, respectively. The kinetics for the homopolymerisation of $\mathbf{1\alpha}$ ($k_{app} = 1.79 \pm 0.09$ h^{-1}) and TMC ($k_{app} = 0.0751 \pm 0.007$ h^{-1}) under the same reaction conditions are shown for comparison. The difference in kinetics of the monomers in the copolymer formation compared to during
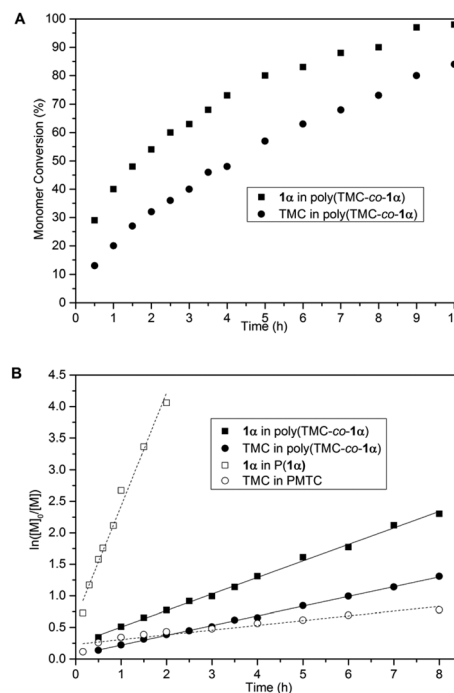
Fig. 6 (A) Monomer conversion as a function of time for $\mathbf{1\alpha}$ and TMC copolymerisation: $f_\alpha/f_{TMC} = 50/50$, $[M_t]_0:[TBD]_0:[BnOH]_0 = 1000:1:1$, rt and $[M_t]_0 = 5$ mol L^{-1} in CH$_2$Cl$_2$. (B) Corresponding kinetic plot for $\mathbf{1\alpha}$ ($y = 0.262x + 0.243$, $R^2 = 0.97$) and TMC ($y = 0.154x + 0.0664$, $R^2 = 0.98$) in the copolymer. The kinetic plots for the homopolymerisation of $\mathbf{1\alpha}$ ($y = 1.79x + 0.64$, $R^2 = 0.98$) and TMC ($y = 0.0751x + 0.232$, $R^2 = 0.96$) are also shown for the same reaction conditions. For the homopolymerisation of $\mathbf{1\alpha}$, time is plotted against $\ln\{([M]_0 - [M]_{eq})/([M] - [M]_{eq})\}$ where $[M]_{eq} = 2.1$ mol L^{-1}. All conversions were determined by ^{1}H NMR spectroscopy from aliquots quenched with benzoic acid.

homopolymerisation further hinted at the formation of a random or alternating copolymer, instead of block copolymers.

For the same 50 : 50 feed ratio, the catalyst and initiator loadings were varied (Table 1, entries 2–5). Generally, good agreement was observed between the SEC estimated and calculated M_n values as for example, in entries 2 and 3. A plot of M_n and Đ (estimated by SEC) as a function of conversion, for a

Table 1 Copolymerization of $\mathbf{1\alpha}$ and TMC with TBD catalyst and BnOH initiator[a]

Entry	$[M_t]_0:[C]_0:[I]_0$	Time (h)	Conv. $\mathbf{1\alpha}$[b] (%)	Conv. TMC[b] (%)	Yield[c] (%)	$M_{n,SEC}$[d] (g mol^{-1})	Đ[d]	$M_{n,calc}$[e] (g mol^{-1})	$M_{n,NMR}$[f] (g mol^{-1})	F_α/F_{TMC}[g]	L_α/L_{TMC}[h]
1[i]	1000 : 1 : 1	3	66	46	64	64 000	1.33	81 100	101 000	56/44	3.03/1.41
2	100 : 1 : 2	0.5	99	96	76	6380	1.19	6870	7320	47/53	1.23/1.46
3	100 : 1 : 1	0.16	69	44	72	8870	1.11	9120	9150	63/37	2.40/1.60
4	400 : 1 : 1	1	97	99	59	43 500	1.63	54 100	53 300	53/47	1.98/1.78
5	800 : 1 : 1	3	96	89	75	59 100	1.44	103 000	107 000	54/46	2.13/1.85

[a] Polymerisation conditions: $f_\alpha/f_{TMC} = 50/50$, $[M_t]_0 = 5$ mol L^{-1} in CH$_2$Cl$_2$, rt. [b] Determined by integration of the crude ^{1}H NMR spectra. [c] Ether-insoluble copolymer (g)/monomer feed (g) × 100. [d] Estimated by SEC (RI detector) *versus* polystyrene standards with CHCl$_3$ eluent. [e] Calculated as: $[M]_0/[I]_0 \times [(M_r(\mathbf{1\alpha}) \times \mathbf{1\alpha}$ conv./100 $\times f_\alpha) + (M_r(TMC) \times$ TMC conv./100 $\times f_{TMC})] + M_r(I)$. [f] Assuming a linear polymer with BnOH and OH end-groups. Based on relative integration of the aromatic resonances of the BnOH initiator ($\sim$7.37 ppm) to the $\mathbf{1\alpha}$ (H-2, 2.30 ppm) and TMC (H-7, 2.05 ppm) repeat units in the ^{1}H NMR spectra (400 MHz, CDCl3) of the copolymer precipitated from ether. [g] Copolymer compositions determined by integration of the ^{1}H NMR spectra of the purified copolymer. [h] $L_\alpha = [I_{\alpha-\alpha}(I_{154.81\ ppm} + I_{154.35} + I_{154.04}) + I_{\alpha-TMC}(I_{154.47})]/I_{\alpha-TMC}(I_{154.47})$ and $L_{TMC} = [I_{TMC-TMC}(I_{154.99\ ppm}) + I_{TMC-\alpha}(I_{154.89})]/I_{TMC-\alpha}(I_{154.89})$ where I = integration of the subscripted carbonate signal in the quantitative ^{13}C NMR spectra. [i] No solvent.

Table 2 Synthesis of poly(TMC-co-**1α**) of different compositions[a]

Entry	f_α/f_{TMC}	**1α** conv.[b] (%)	TMC conv.[b] (%)	$M_{n, SEC}$[c] (g mol^{-1})	$Đ$[c]	$M_{n, calc}$[d] (g mol^{-1})	Yield[e] (%)	F_α/F_{TMC}[f]	L_α/L_{TMC}[g]
1	100/0	60	—	25 600[h]	1.41	41 900	48	—	—
2	90/10	73	99	33 200	1.74	49 900	57	93/7	—
3	80/20	81	99	36 100	1.61	53 300	69	85/15	3.30/0.80
4	70/30	88	97	39 300	1.64	54 900	54	66/34	1.97/1.13
5	60/40	98	99	36 700	1.46	57 200	43	60/40	2.03/1.64
6	50/50	97	99	43 500	1.63	54 100	59	53/47	1.98/1.78
7	40/60	99	98	30 200	1.75	51 700	66	39/61	1.65/2.79
8	30/70	99	96	26 100	1.39	48 200	53	31/69	1.27/2.91
9	20/80	99	99	46 500	1.65	46 200	76	23/77	—
10	10/90	99	99	40 900	1.37	43 400	69	14/86	—
11	0/100	—	99	42 500	1.55	40 500	72	—	—

[a] Polymerisation conditions: $[M_t]_0 = 5$ mol L^{-1} in CH$_2$Cl$_2$, $[M_t]_0 : [TBD]_0 : [BnOH]_0 = 400 : 1 : 1$, 1 h, rt. [b] Determined by integration of the crude ^{1}H NMR spectra (CDCl$_3$). [c] Estimated by SEC (RI detector) versus polystyrene standards in CHCl$_3$ eluent. [d] Calculated as: $[M]_0/[I]_0 \times [(M_r(1\alpha) \times \alpha$ conv./$100 \times f_\alpha) + (M_r(TMC) \times TMC$ conv./$100 \times f_{TMC})] + M_r(I)$. [e] Ether-insoluble copolymer (g)/monomer feed (g) × 100. [f] Copolymer compositions determined by integration of the ^{1}H NMR spectra of the purified copolymer. [g] $L_\alpha = [I_{\alpha-\alpha}(I_{154.81 ppm} + I_{154.35} + I_{154.04}) + I_{\alpha-TMC}(I_{154.47})]/I_{\alpha-TMC}(I_{154.47})$ and $L_{TMC} = [I_{TMC-TMC}(I_{154.99 ppm}) + I_{TMC-\alpha}(I_{154.89})]/I_{TMC-\alpha}(I_{154.89})$ where I = integration of the subscripted carbonate signal in the quantitative ^{13}C NMR spectra. [h] Estimated by SEC (RI detector) versus PMMA standards with HFIP eluent.

copolymerisation carried out with 0.1 mol% TBD and $[M_t]_0/[I]_0$ of 50, showed a linear increase in molecular weight with total monomer conversion whilst maintaining relatively narrow dispersities ($Đ < 1.2$) (Fig. S21†). This indicated a well-controlled polymerisation under these conditions. At lower catalyst and initiator loading (0.125 mol%), a greater disparity between the theoretical M_n and the one determined by SEC was observed (entry 5).

Subsequently, the feed ratio of the two co-monomers was varied for $[M_t]_0/[I]$ of 400 (Table 2). The copolymers were all soluble in typical organic solvents, namely CHCl$_3$, CH$_2$Cl$_2$ and THF, though this solubility was reduced for copolymers of higher **1α** content of 85 and 93 mol%. Monomer conversion and the resulting copolymer composition were determined by integration of the methylene H-2 proton environments of **1α** and TMC. Nearly full conversion (>96%) was observed for the TMC co-monomer in all cases. For **1α**, full or high conversion (>88%) was observed within the 1 h reaction time for **1α** and TMC feed ratios (f_α/f_{TMC}) up to 70/30. At higher ratios (Table 2, entries 2 and 3), the polymerisation solution became cloudy as in the homopolymerisation of **1α**. Nevertheless, ^{1}H NMR spectroscopy of the purified polymers revealed copolymer compositions well correlated to the input ratio of co-monomers, which is advantageous for polymer design and tunability. Molecular weights were also estimated by SEC and high M_n (up to 46 500 g mol^{-1}) were achieved after 1 h, with generally good agreement with the M_n predicted from monomer conversion.

Copolymer structure

^{1}H NMR analysis of poly(TMC-co-53 mol%-**1α**) (Table 2, entry 6) revealed proton environments analogous to those observed in the NMR spectra of PTMC and poly(TMC-co-93 mol%-**1α**) (Fig. 7). By displaying a unique diffusion coefficient (Fig. S17†), DOSY NMR confirmed the presence of a copolymer rather than two homopolymers, as poly(**1α**) would also be insoluble in the CDCl$_3$ solvent.
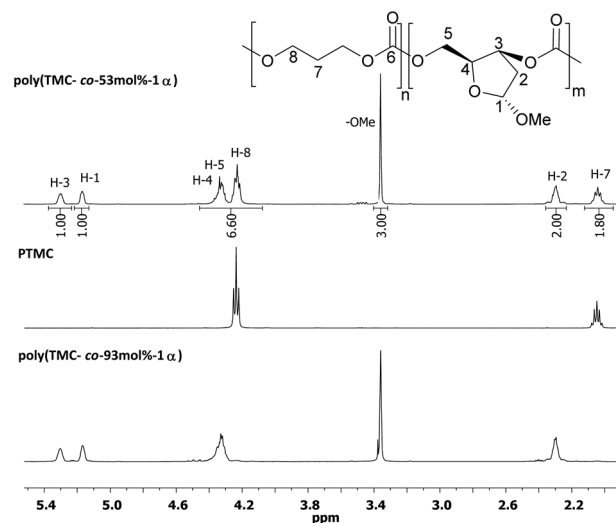

Fig. 7 ^{1}H NMR spectra (400 MHz, CDCl$_3$) of poly(TMC-co-53 mol%-**1α**), poly(TMC-co-93 mol%-**1α**) and PTMC.

Insight into the copolymer chain microstructure was gained by ^{13}C{^{1}H} NMR spectroscopy. Specifically, detailed analysis of the carbonyl region revealed 6 carbonate environments (Fig. 8). These were assigned based on comparison with the homopolymer NMR spectra and their relative intensity depending on co-monomer content. Carbonate environments at 154.89 and 154.47 ppm were assigned to alternating TMC-α and α-TMC linkages, respectively, and were most intense for the copolymer with 53 mol% **1α** content (Fig. 8B). The presence of a TMC–TMC carbonate environment and the TT, HT and HH regiochemistries characteristic of **1α** linkages also indicated formation of **1α** and TMC segments. Thus, the copolymers were not perfectly alternating, which was consistent with the slightly faster consumption of **1α**.
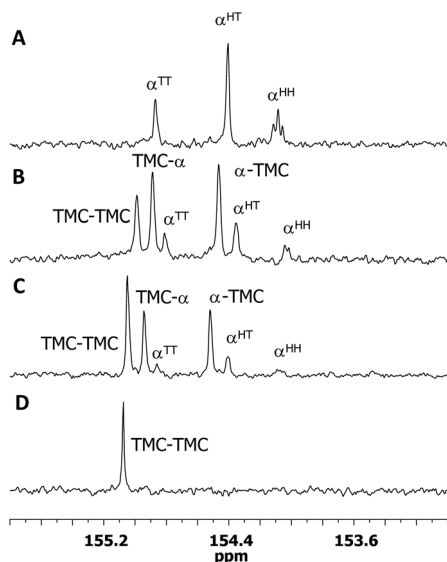
Fig. 8 Carbonate region of the $^{13}C\{^1H\}$ NMR spectra (400 MHz, CDCl$_3$) of (A) poly(TMC-*co*-93 mol%-**1α**), (B) poly(TMC-*co*-53 mol%-**1α**), (C) poly(TMC-*co*-31 mol%-**1α**) and (D) PTMC.
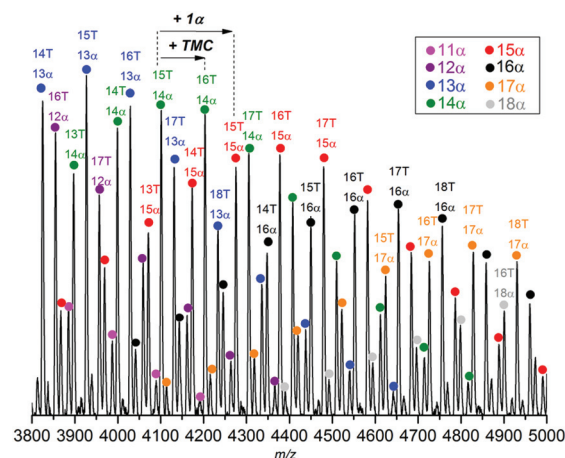

Fig. 9 MALDI-ToF MS of poly(TMC-*co*-47 mol%-**1α**) (Table 1, entry 2). *m/z* values are consistent with the sodium adduct of the copolymer with benzyl alcohol and OH end-groups (see Fig. S30† for details). Colours highlight peaks with the same number of **1α** units but different amounts of TMC (T).

The average lengths of these segments ($L_α$ and L_{TMC}) were estimated based on the relative integration of these carbonyl signals by quantitative $^{13}C\{^1H\}$ NMR spectroscopy (Tables 1 and 2). Short $L_α$ lengths, even at 85 mol% **1α** content (3.30, Table 2, entry 3), indicated that blocky copolymers were not being formed. Estimation of the reactivity ratios using the Finemann–Ross method[39] for polymerisations with monomer conversions less than 15% gave values for **1α** and TMC, respectively of $r_α$ = 0.54 ± 0.08 and r_{TMC} = 0.41 ± 0.01 (Fig. S22†). These values, both less than 1 suggest a random copolymer (rr = 1) tending towards alternating (rr = 0). Attempts to synthesise di-, tri- and tetra-block copolymers by sequential addition of monomers proved challenging due to the lack of copolymer solubility when blocks of **1α** were present. Further complexity arose from the thermodynamically limited equilibrium homopolymerisation of **1α**, which resulted in less than full conversion and prevented clean **1α**-TMC block sequence.

MALDI-ToF MS (Fig. 9 and S30†) of poly(TMC-*co*-47 mol%-**1α**) (Table 1, entry 2) showed multiple polymer series consisting of **1α** and TMC repeat units (*m/z* 174 and 102, respectively). All peaks were assigned to sodium adducts of copolymers with benzyl alcohol and OH end-groups. The majority had roughly equal numbers of **1α** and TMC units as expected based on the copolymer composition determined by NMR spectroscopy. In Fig. 9, polymer series have been differentiated and labelled so that a series contains the same number of **1α** units (*m* = 11–18) but different numbers of TMC co-monomer (*n* = 11–22). This is arbitrary and not representative of the polymerisation process, as from most signals, a higher *m/z* species can be found that corresponds to the addition of either a TMC or **1α** unit.

For example, the species at *m/z* ~ 4100 (consistent with a polymer chain with 15 TMC and 14 **1α** units) could grow by a

1α unit to *m/z* ~ 4275 (15T, 15α) or by a TMC unit to *m/z* ~ 4200 (16T, 14α). The presence of all possible combinations supports the random, statistical nature of the copolymers.

Despite its lack of homopolymerisation, **1β** could be copolymerised with TMC using TBD catalyst and alcohol initiator under the same reaction conditions of rt and [M$_t$]$_0$ of 5 mol L^{-1} in CH$_2$Cl$_2$. For a 50 : 50 feed ratio of **1β** : TMC, full TMC conversion was achieved but, conversely to the copolymerisation of **1α** with TMC, conversions of **1β** greater than 40% were not observed. Monitoring conversion *versus* time (Fig. S23†) for a polymerisation carried out with 0.1 mol% TBD and [M$_t$]$_0$/[I]$_0$ of 1000 showed the faster consumption of TMC compared to **1β**. Compared to the copolymerisation of TMC with the α-anomer, the corresponding kinetic plot (Fig. S24†) gave significantly lower values for k_{app} of 0.0145 ± 0.0009 h^{-1} and 0.0621 ± 0.002 h^{-1} for **1β** and TMC, respectively. $^{13}C\{^1H\}$ NMR analysis (Fig. S19†) of the copolymer ($F_β/F_{TMC}$ = 32/68, $M_{n,SEC}$ = 43 200 g mol^{-1}, Đ 1.39) revealed no signals due to the HH, HT and TT linkages of **1β** segments. This is consistent with no homopolymerisation of **1β** being observed under these reaction conditions. Thus, **1α** can ring-open **1α** and TMC but will not polymerise with **1β**, whereas TMC will copolymerise with both **1β** and **1α**.

(Co)polymer thermal properties

Differential scanning calorimetry (DSC) of the copolymers showed a single T_g supportive of a random or alternating rather than block copolymers. The homopolymer of **1α** exhibited a significantly lower T_g of ~58 °C, compared to previously reported sugar-based polycarbonates derived from D-glucose[25] (T_g = 122 °C), D-mannose[24] (T_g = 152 °C) and D-xylose[26] (T_g = 128 °C). As well as the presence of pyranose or furanose rings in the polymer backbone, these contain additional *O*-methoxy and ketal protecting groups that further restrict rotation about

the main chain leading to increased T_g values. For further comparison, a T_g of 84.5 °C has been reported for poly(cyclopentene carbonate) produced by cyclopentene oxide and CO_2 copolymerisation.[40]

An increase in **1α**-content led to an increase in the T_g of the copolymer (Table 3). In general, good agreement with the Fox equation was observed allowing for tailoring of the polymer properties. Small exotherms at ~137 °C were also observed in the cooling curves (and corresponding endotherms in the heating curve) for copolymers with greater than 23 mol% of **1α** (Fig. 10). These are potentially due to crystallisation (and melting) of crystalline domains. Nevertheless, no crystallinity was observed by powder X-ray diffraction (Fig. S35†).

Thermogravimetric analysis (TGA) of the copolymers of various compositions revealed a general trend towards lower thermal stability with higher **1α** content (Fig. 10 And Table 4). For example, the temperature at which the maximum % mass loss was observed (T_{inf}) occurred at ~195 °C for the copolymer with 93 mol% **1α** and increased to ~212 °C for 14 mol% **1α**. The onset of thermal degradation (T_{on}) was observed at ~170 °C for copolymers of high sugar content (66–93 mol%) and showed less stepwise degradation profiles (Fig. 11) com-

Table 3 DSC data for poly(TMC-*co*-α) of different composition

Entry	α (mol%)	T_g (°C)	T_g^{calc} (°C)	T_c (°C)	ΔH_c (J g^{-1})
1	100	58	—	137.3	0.301
2	93	50	51	137.0	0.512
3	85	46	48	—	—
4	66	38	34	137.1	1.96
5	53	30	24	138.4	0.786
6	37	9	11	137.0	0.937
7	31	3	5	137.2	2.46
8	23	−3	−2	137.6	1.50
9	14	−11	−11	—	—
10	0	−25	—		
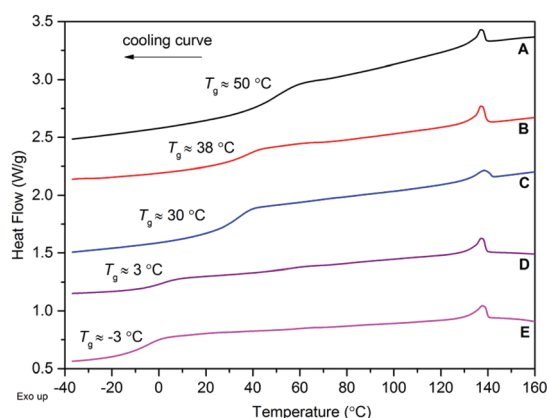
Fig. 10 Selected DSC traces of **1α** and TMC copolymers showing the cooling curve from 160 to −40 °C (10 K min^{-1}) of the first heating cycle. A: poly(TMC-*co*-93 mol%-**1α**); B: poly(TMC-*co*-66 mol%-**1α**); C: poly(TMC-*co*-53 mol%-**1α**); D: poly(TMC-*co*-31 mol%-**1α**); E: poly(TMC-*co*-23 mol%-**1α**).

Table 4 TGA data for copolymers of TMC and **1α** with different compositions

Entry	α (mol%)	T_{on}^{a} (°C)	T_{inf}^{b} (°C)	% Mass loss^{c}
1	100	125	200	94
2	93	156	195	93
3	85	160	196	98
4	66	168	204	91
5	53	196	205	97
6	31	194	210	98
7	23	197	212	97
8	14	196	212	90
9	0	197	213	96

^{a} Onset of thermal degradation. ^{b} Temperature at which maximum mass loss is observed. ^{c} Total mass loss.
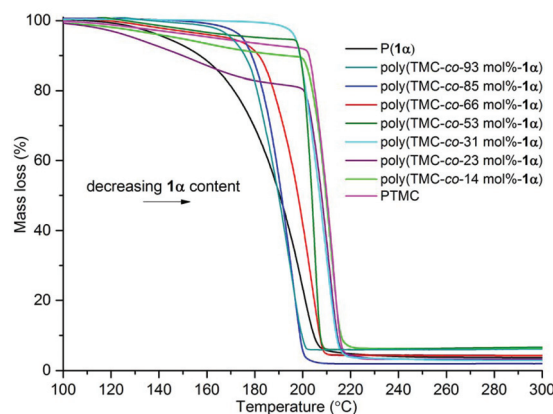

Fig. 11 TGA analysis of poly(TMC-*co*-**1α**) of various composition. Copolymers were heated from 30–500 °C at 5 K min^{-1}.

pared to copolymers of 53 mol% or less **1α** content which began to show mass loss at ~200 °C. For all copolymers, mass losses of 90% or over were observed. Analysis of the degradation products by tandem mass spectrometry detected ions of m/z 44 attributed to the loss of CO_2^{+} (Fig. S31†).

Conclusions

In conclusion, a three-step synthesis for the preparation of novel 6-membered *cis*-configured cyclic carbonate monomers, derived from natural sugar 2-deoxy-D-ribose and CO_2, is reported. The –OMe substituted α- and β-anomers displayed markedly different ROP reactivity, which was rationalised by DFT modelling and the calculation of their respective ring strains. While the β-anomer could not be polymerised under the conditions trialled, homo-polymerisation of the α-anomer using an organocatalytic approach resulted in novel polycarbonates which were characterised by NMR, SEC and MALDI-ToF. Copolymerisation of the α-anomer with TMC resulted in high M_n aliphatic polycarbonates with controlled and high sugar content. T_g values of these random copolymers could be tuned

over a wide window of −25 to +58 °C and thermal degradability enhanced with increasing sugar content. Further work will look to exploit the huge functionalisation potential of the anomeric substituent for the design of new sugar-based polymers with desirable properties. This work also presents the opportunity to develop dedicated catalytic systems to control further the monomer reactivity and the microstructure of these new APCs.

Experimental

Methods and instrumentation

All NMR spectra were recorded in CDCl$_3$ or 1,1,1,3,3,3-hexafluoroisopropanol-d$_2$ (HFIP-d$_2$) on a Bruker-400 or 500 instrument and referenced to residual solvent peaks: ^{1}H NMR spectra δ_H = 7.26 (CDCl$_3$), 4.86 (HFIP-d$_2$); ^{13}C{^{1}H} spectra δ_C = 77.16 (CDCl$_3$) and 68.07 ppm (HFIP-d$_2$); CHN microanalysis was performed by Mr Stephen Boyer of the London Metropolitan University. Mass spectrometry were recorded with a microToF electrospray time-of-flight (ESI-ToF) mass spectrometer (Bruker Daltonik) in methanol. Infra-red spectra were recorded as thin films on a PerkinElmer 1600 Fourier transform spectrometer. Number-average molecular weights (M_n) and dispersities Đ (M_w/M_n) were estimated by size exclusion chromatography (SEC) with a differential refractive index (RI) detector. For polymeric materials, soluble in CHCl$_3$, samples were dissolved at a concentration of 2 mg mL^{-1} and the 1260 SEC MDS system from Agilent used with a PL gel 5 μm mixed-D 300 × 7.5 mm column, calibrated with a set of polystyrene standards. HPLC grade CHCl$_3$ was flowed at a rate of 1 mL min^{-1} and the detector maintained at 35 °C. For polymers only soluble in HFIP, a Polymer Laboratories PL-GPC 50 integrated system was used with 2 × PL HFIPgel columns (maintained at 40 °C) and calibrated to PMMA standards. DSC analysis was recorded on a TA Instruments DSC Q20. Samples were rapidly cooled to −40 °C and then heated to 200 °C at a rate of 10 K min^{-1} before being cooled back to −40 °C at the same rate. A second heating and cooling cycle was carried out following completion of the first. A Setsys Evolution TGA 16/18 from Setaram was used for thermogravimetric analysis (TGA). The sample was heated under an argon flow (20 mL min^{-1}) from 30 to 500 °C at a rate of 5 K min^{-1}. Evolving gas was analysed by a Omnistar GSD 320 mass spectrometer equipped with a quadrupole mass analyser and SEM detector. Matrix-assisted laser desorption ionization-time of flight (MALDI-ToF) mass spectrometry was conducted using a Bruker Autoflex speed MALDI Mass Spectrometer with a 2 kHz Smartbeam-II laser. A solution of trans-2-[3-(4-tert-butylphenyl)-2-methyl-2-propenylidene]malononitrile (DCTB) matrix in CHCl$_3$ (10 mg mL^{-1}) was added to CHCl$_3$ solutions of polymer (5 mg mL^{-1}) with sodium trifluoroacetate (0.1 mol L^{-1} in HFIP) in a 25 : 5 : 1 ratio, and the samples centrifuged for 1 min. ~1–2 μL of the solution was spotted onto a polished steel MALDI plate and positive ion MALDI spectra obtained in reflector mode with varying laser intensity. Single-crystal X-ray

diffraction analysis was carried out by Dr Gabriele Kociok-Köhn on a Nonius Kappa CCD diffractometer using Cu-K$_\alpha$ radiation (λ = 1.54184 Å) at 150 K. Powder diffraction patterns were recorded by Mr Alan Carver on a Bruker Advance D8 diffractometer with copper K$_\alpha$ radiation (λ = 1.5406 Å) at 298 K. Data was recorded from a 2θ of 4 to 60° with 0.02 steps per s and 0.5 s per step.

Computational details

All DFT calculations were performed using the Gaussian09 suite of codes (revision D.01)[41] and geometries fully optimised using the rωB97XD LC hybrid functional developed by Chai and Head-Gordon.[42] For modelling of the ROP initiation step, a split-valence triple ζ with polarization and diffuse functions, 6-311++G(d, p) basis set was employed for the carbonate, guanidine and alcohol moieties of **1α/β** or TMC, TBD and BnOH, respectively. A lower, split-valence double ζ 6-31+G(d) basis set was applied to all other atoms. For ring strain calculations, a 6-311++G(2d, p) basis was employed. All calculations were carried out using a temperature of 298 K and solvent effects in dichloromethane considered using a conductor-like polarisable continuum model (CPCM).[43] The nature of all the stationary points as minima or transition states was verified by calculations of the vibrational frequency spectrum. All transition states were characterised by precisely one imaginary mode corresponding to the intended reaction. Free energies were calculated within the harmonic approximation for vibrational frequencies.

Syntheses

2-Deoxy-D-ribose was purchased from Carbosynth and used without further purification. TMC was prepared following the literature procedures,[22c,44] recrystallised from dry ether and stored in a glovebox. TBD (Sigma Aldrich) was dried over CaH$_2$ and stored in a glovebox immediately prior to use. Benzyl alcohol (Sigma Aldrich) was distilled over CaH$_2$ before being stored in a glovebox. Dry diethyl ether and toluene were obtained from an MBraun solvent purification system (SPS) and stored over 3 Å molecular sieves. N4.5 CP grade CO$_2$ was purchased from BOC and introduced using standard Schlenk line techniques. Column chromatography was performed on silica gel (Sigma Aldrich, 200–400 mesh particle size, 60 Å pore size) and spots visualised with KMnO$_4$ solution. All R_f values refer to a 1 : 1 CHCl$_3$: acetone eluent. All other reagents were purchased from either Sigma Aldrich or Alfa Aesar and used without further purification.

1-O-Methyl-2-deoxy-3-tosyl-5-TBDMS-D-ribofuranoside (3). In a modified literature procedure,[45] conc. HCl (4 drops) was added to a stirring solution of 2-deoxy-D-ribose (5.00 g, 37.2 mmol) in methanol (60 ml). After 30 minutes, the reaction was quenched by addition of anhydrous pyridine (2 ml) and volatiles removed in vacuo. To the resulting oil and a catalytic amount of DMAP (0.488 g, 3.72 mmol), in anhydrous pyridine (40 ml), was added TBDMSCl (6.02 g, 40.0 mmol) portion wise. After 2 h stirring at 25 °C, TsCl (7.64 g, 40.0 mmol) was added and the reaction mixture stirred for a

further 12 h before being quenched with methanol (4 ml). Following the removal of volatiles under reduced pressure, the crude product was purified *via* a silica plug with CH_2Cl_2 eluent to afford a colourless oil (12.7 g, 82%, mixture of α- and β-anomers). R_f 0.75; ^{1}H NMR (400 MHz, CDCl₃, 25 °C): δ_H (ppm) 7.78 (4H, d, *J* 8.1 Hz, ArH, α + β), 7.33 (4H, d, *J* 8.1 Hz, ArH, α + β), 5.09 (1H, dd, *J* 5.4, 3.3 Hz, H-1α), 5.03–5.00 (2H, m, H-3α, H-1β), 4.95 (1H, ddd, *J* 7.6, 2.9, 1.8 Hz, H-3β), 4.21 (1H, dd, *J* 5.4, 2.6 Hz, H-4β), 4.10–4.06 (1H, m, H-4α), 3.63 (2H, dd, *J* 11.3, 2.8 Hz, H-5β), 3.55 (1H, dd, *J* 10.7, 5.2 Hz, H-5α), 3.47 (1H, dd, *J* 10.7, 6.8 Hz, H-5′α), 3.34 (3H, s, β-OMe), 3.30 (s, 3H, α-OMe), 2.44 (6H, s, TsMe, α + β), 2.30 (1H, ddd, *J* 14.5, 5.4, 4.1 Hz, H-2α), 2.20–2.12 (2H, m, H-2′, α + β), 2.04, (1H, d, *J* 14.4 Hz, H-2β), 0.84 (18H, s, *t*Bu-Si, α + β), 0.00 (12H, s, 6H, Me₂Si, α + β); ${}^{13}C\{{}^{1}H\}$ NMR (101 MHz, CDCl₃, 25 °C) δ_C (ppm) 145.1, 145.0, 133.9, 133.7 (ArC, α + β), 130.1, 130.0, 128.0, 128.0 (ArCH, α + β), 105.3, 105.1 (C-1, α + β), 84.1, 83.8 (C-3, α + β), 81.7, 80.4 (C-4, α + β), 63.3, 62.6 (C-5, α + β), 55.6, 55.1 (OMe, α + β), 39.6, 39.3 (C-2, α + β), 25.9 (*t*BuSi, α + β), 21.8, 18.4 (TsMe, α + β), −5.3, −5.4, −5.4, −5.5 (Me₂Si, α + β); Found: C, 54.82; H, 7.75. $C_{19}H_{32}O_6SSi$ requires C, 54.78; H, 7.74%; HR-MS (ESI) $[C_{19}H_{32}O_6SSi + Na]^+$ Theo. 439.1581 found 439.1593 *m/z*.

1-*O*-Methyl-2-deoxy-3-tosyl-D-ribofuranoside (2). Following the procedure reported by Vaino and Szarek[46] iodine (3.0 g, 1 wt%) was added to a 0.1 mol L⁻¹ solution of **3** (12.7 g, 28.8 mmol) in methanol (300 ml) and the reaction mixture heated to reflux for 4 h. After cooling to rt, excess iodine was quenched with Na₂S₂O₃ until colourless and volatiles removed under reduced pressure. The resulting residue was extracted into EtOAc, washed with water and the organic layer dried over MgSO₄ to afford the product as a colourless oil (7.19 g, 78%, mixture of α- and β-anomers): ^{1}H NMR (400 MHz, CDCl₃, 25 °C), δ_H (ppm) 7.78 (4H, d, *J* 8.3 Hz, ArH, α + β), 7.36 (4H, d, *J* 8.3 Hz, ArH, α + β), 5.12 (1H, dd, *J* 5.6, 2.6 Hz, H-1α), 5.08 (1H, ddd, *J* 6.8, 4.2, 2.7 Hz, H-3α), 5.03 (1H, dd, *J* 5.2, 1.0 Hz, H-1β), 4.91 (1H, ddd, *J* 8.4, 4.2, 2.4 Hz, H-3β), 4.31 (1H, dd, *J* 2.9, 2.7 Hz, H-4α), 4.21 (1H, dd, *J* 7.1, 3.1 Hz, H-4β), 3.76 (1H, ddd, *J* 12.2, 4.3, 2.9 Hz, H-5β), 3.63 (1H, ddd, *J* 12.4, 3.0, 2.9 Hz, H-5α), 3.49 (1H, ddd, *J* 12.4, 10.2, 2.9 Hz, H-5′α), 3.60–3.49 (1H, m, H-5′β), 3.37 (3H, s, α-OMe), 3.35 (3H, s, β-OMe), 2.73 (1H, dd, *J* 10.2, 3.0 Hz, 5-α-OH), 2.45 (6H, s, TsMe, α + β), 2.30 (1H, ddd, *J* 15.0, 5.6, 4.2 Hz, H-2α), 2.24 (1H, ddd, *J* 15.0, 7.1, 2.5 Hz, H-2′α), 2.03 (2H, ddd, *J* 14.7, 2.4, 1.1, H-2β), 1.74 (1H, dd, *J* 8.5, 4.4 Hz, 5-β-OH). ${}^{13}C\{{}^{1}H\}$ (101 MHz, CDCl₃, 25 °C), δ_C (ppm) 145.4, 145.2 (Ar, α + β), 133.3, 133.7 (Ar, α + β), 130.2, 130.1, 128.1, 128.0 (ArC, α + β), 105.4, 104.8 (C-1, α + β), 85.7, 82.7 (C-3, α + β), 81.3, 79.6 (C-4, α + β), 63.3, 61.7 (C-5, α + β), 55.8, 55.1 (OMe, α + β), 40.5, 39.7 (C-2, α + β), 21.8, 21.2 (TsMe, α + β); Found: C, 51.65; H, 6.07. $C_7H_{10}O_5$ requires C, 51.64; H, 6.00%; HR-MS (ESI) $[C_{13}H_{18}O_6S + Na]^+$ Theo. 325.0721 found 325.0743 *m/z*.

1-*O*-Methyl-2-deoxy-D-ribofuranoside-3,5-*O*-*cis*-cyclic carbonate (1). A solution of **2** (7.06 g, 23.4 mmol) in anhydrous acetonitrile (230 ml, 0.1 mol L⁻¹) was saturated with CO₂ at 0 °C in an ice-water bath. Under a stream of CO₂, DBU (3.5 ml,

23.4 mmol) was added dropwise and the solution allowed to warm to rt. After 48 h volatiles were removed under reduced pressure and the crude reaction mixture immediately subject to flash column chromatography (CHCl₃ to 1% acetone/CHCl₃ eluent). The α-rich fraction was recrystallised from dry ether to afford pure **1α** as large colourless needles (1.55 g, 38%). R_f 0.57; Mpt 67–68 °C; ^{1}H NMR (400 MHz, CDCl₃, 25 °C, Fig. S1†) δ_H (ppm) 5.22 (1H, dd, *J* 5.2, 2.6 Hz, H-1), 5.13 (1H, ddd, *J* 6.3, 4.9, 3.0 Hz, H-3), 4.48 (2H, qd, *J* 12.4, 2.1 Hz, H-5), 4.39 (1H, dt, *J* 4.9, 2.1 Hz, H-4), 3.37 (3H, s, OMe), 2.42 (1H, ddd, *J* 15.1, 5.2, 3.0 Hz, H-2), 2.36 (1H, ddd, *J* 15.1, 6.3, 2.6 Hz, H-2′); ${}^{13}C\{{}^{1}H\}$ (101 MHz, CDCl₃, 25 °C, Fig. S2†) δ_C (ppm) 148.5 (C=O), 104.6(C-1), 80.8 (C-3), 70.3 (C-4), 67.0 (C-5), 55.7 (OMe), 42.0 (C-2); Found: C, 48.28; H, 5.82. $C_7H_{10}O_5$ requires C, 48.45; H, 5.79%; HR-MS (ESI) $[C_7H_{11}O_5]^+$ Theo. 175.060648 found 175.0609 *m/z*; FTIR (thin film) 1744 cm⁻¹ (C=O). The β-rich fraction was recrystallised from hot toluene to afford white needles of **1β** (1.71 g, 42%). R_f 0.47; Mpt 106–108 °C. ^{1}H NMR (400 MHz, CDCl₃, 25 °C, Fig. S6†) δ_H (ppm) 5.15–5.04 (2H, m, H-1, H-3), 4.51 (1H, dt, *J* 5.7, 1.8 Hz, H-4), 4.37 (1H, dd, *J* 12.3, 1.8 Hz, H-5), 4.32 (1H, ddd, *J* 12.3, 1.8, 0.5 Hz, H-5′), 3.30 (3H, s, OMe), 2.39 (1H, d, *J* 14.6 Hz, H-2), 2.17 (1H, ddd, *J* 14.6, 5.6, 4.9 Hz, H-2′); ${}^{13}C\{{}^{1}H\}$ NMR (101 MHz, CDCl₃, 25 °C, Fig. S7†) δ_C (ppm) 149.0 (C=O), 104.3 (C-1), 80.7 (C-3), 73.6 (C-4), 66.8 (C-5), 54.7 (OMe), 41.2 (C-2); Found: C, 48.27; H, 5.89. $C_7H_{10}O_5$ requires C, 48.45; H, 5.79%; HR-MS (ESI) $[C_7H_{10}O_5 + Na]^+$ Theo. 197.042593 found 197.0451 *m/z*; FTIR (thin film) 1741 cm⁻¹ (C=O).

General polymerization and copolymerisation procedure. To **1α** (174 mg, 1 mmol) and TMC (102 mg, 1 mmol) in CH₂Cl₂ (0.34 ml, 5 mol L⁻¹) was added BnOH (40 μL, 0.04 mmol, 1 mol L⁻¹ in CH₂Cl₂) followed by TBD (20 μL, 0.02 mmol, 1 mol L⁻¹ in CH₂Cl₂) and the reaction stirred at rt. The polymerisation was quenched by addition of excess benzoic acid and the polymer isolated as a white powder by precipitation from ether (210 mg, 76%); poly(TMC-*co*-47 mol%-α): ^{1}H NMR (400 MHz, CDCl₃, 25 °C, Fig. S12†): δ_H (ppm) 5.39–5.23 (1H, m, H-3), 5.17 (1H, m, H-1), 4.36–4.31 (3H, m, H-4, H-5), 4.26–4.22 (4.5H, m, H-8), 3.37 (3H, s, OMe), 2.37–2.22 (2H, m, H-2), 2.05 (2.25H, q, *J* 6.2 Hz, H-7). ${}^{13}C\{{}^{1}H\}$ NMR (101 MHz, CDCl₃, 25 °C, Fig. S15†): δ_C (ppm) 155.1, 155, 154.9, 154.5, 154.4, 154.1 (C=O), 104.2 (C-1), 76.4 (C-3), 76.3 (C-4) 64.8 (C-5), 64.6 (C-8), 55.6 (OMe), 40.5 (C-2), 28.2 (C-7); $M_{n,SEC}$ 6380 g mol⁻¹ (*Đ* 1.19); FTIR (thin film) 1741 cm⁻¹ (C=O).

Acknowledgements

Notes and references

1 (a) A. Llevot, P.-K. Dannecker, M. von Czapiewski, L. C. Over, Z. Söyler and M. A. R. Meier, *Chem. – Eur. J.*, 2016, **22**, 11510–11521; (b) C. K. Williams and M. A. Hillmyer, *Polym. Rev.*, 2008, **48**, 1–10; (c) M. J. L. Tschan, E. Brule, P. Haquette and C. M. Thomas, *Polym. Chem.*, 2012, **3**, 836–851; (d) A. Pellis, E. Herrero Acero, L. Gardossi, V. Ferrario and G. M. Guebitz, *Polym. Int.*, 2016, **65**, 861–871; (e) A. Gandini and T. M. Lacerda, *Prog. Polym. Sci.*, 2015, **48**, 1–39.

2 J. Feng, R.-X. Zhuo and X.-Z. Zhang, *Prog. Polym. Sci.*, 2012, **37**, 211–236.

3 (a) N. G. Ricapito, C. Ghobril, H. Zhang, M. W. Grinstaff and D. Putnam, *Chem. Rev.*, 2016, **116**, 2664–2704; (b) G. L. Gregory, E. M. Lopez-Vidal and A. Buchard, *Chem. Commun.*, 2017, **53**, 2198–2217; (c) J. A. Galbis and M. G. García-Martín, *Top. Curr. Chem.*, 2010, **295**, 147–176; (d) J. A. Galbis and M. G. García-Martín, in *Monomers, Polymers and Composites from Renewable Resources*, ed. M. N. Belgacem and A. Gandini, Elsevier, Oxford, 2008, pp. 89–114; (e) J. A. Galbis, M. D. G. García-Martín, M. V. de Paz and E. Galbis, *Chem. Rev.*, 2015, **116**, 1600–1636; (f) X. Feng, A. J. East, W. B. Hammond, Y. Zhang and M. Jaffe, *Polym. Adv. Technol.*, 2011, **22**, 139–150.

4 (a) F. Fenouillot, A. Rousseau, G. Colomines, R. Saint-Loup and J. P. Pascault, *Prog. Polym. Sci.*, 2010, **35**, 578–622; (b) C. Lavilla, A. Alla, A. Martínez de Ilarduya and S. Muñoz-Guerra, *Biomacromolecules*, 2013, **14**, 781–793; (c) C. Japu, A. Martinez de Ilarduya, A. Alla, M. G. Garcia-Martin, J. A. Galbis and S. Munoz-Guerra, *Polym. Chem.*, 2013, **4**, 3524–3536.

5 D. Cunliffe, S. Pennadam and C. Alexander, *Eur. Polym. J.*, 2004, **40**, 5–25.

6 (a) E. S. Place, J. H. George, C. K. Williams and M. M. Stevens, *Chem. Soc. Rev.*, 2009, **38**, 1139–1151; (b) C. K. Williams, *Chem. Soc. Rev.*, 2007, **36**, 1573–1580.

7 (a) S. Tempelaar, L. Mespouille, O. Coulembier, P. Dubois and A. P. Dove, *Chem. Soc. Rev.*, 2013, **42**, 1312–1336; (b) W. Chen, F. Meng, R. Cheng, C. Deng, J. Feijen and Z. Zhong, *J. Controlled Release*, 2014, **190**, 398–414.

8 W. Zhu, X. Huang, C. Li, Y. Xiao, D. Zhang and G. Guan, *Polym. Int.*, 2011, **60**, 1060–1067.

9 Q. Li, W. Zhu, C. Li, G. Guan, D. Zhang, Y. Xiao and L. Zheng, *J. Polym. Sci., Part A: Polym. Chem.*, 2013, **51**, 1387–1397.

10 A. T. Lonnecker, Y. H. Lim, S. E. Felder, C. J. Besset and K. L. Wooley, *Macromolecules*, 2016, **49**, 7857–7867.

11 S. Paul, Y. Zhu, C. Romain, R. Brooks, P. K. Saini and C. K. Williams, *Chem. Commun.*, 2015, **51**, 6459–6479.

12 (a) S. M. Guillaume and J.-F. Carpentier, *Catal. Sci. Technol.*, 2012, **2**, 898–906; (b) G. Rokicki and P. G. Parzuchowski, in *Polymer Science: A Comprehensive Reference*, ed. K. Matyjaszewski and M. Möller, Elsevier, Amsterdam, 2012, pp. 247–308.

13 (a) M. Helou, O. Miserque, J.-M. Brusson, J.-F. Carpentier and S. M. Guillaume, *ChemCatChem*, 2010, **2**, 306–313; (b) N. Ajellal, J.-F. Carpentier, C. Guillaume, S. M. Guillaume, M. Helou, V. Poirier, Y. Sarazin and A. Trifonov, *Dalton Trans.*, 2010, **39**, 8363–8376.

14 B. Lin and R. M. Waymouth, *J. Am. Chem. Soc.*, 2017, **139**, 1645–1652.

15 (a) A. P. Dove, R. C. Pratt, B. G. G. Lohmeijer, R. M. Waymouth and J. L. Hedrick, *J. Am. Chem. Soc.*, 2005, **127**, 13798–13799; (b) X. Zhang, G. O. Jones, J. L. Hedrick and R. M. Waymouth, *Nat. Chem.*, 2016, **8**, 1047–1053.

16 V. Ladelta, P. Bilalis, Y. Gnanou and N. Hadjichristidis, *Polym. Chem.*, 2017, **8**, 511–515.

17 J. Liu, S. Cui, Z. Li, S. Xu, J. Xu, X. Pan, Y. Liu, H. Dong, H. Sun and K. Guo, *Polym. Chem.*, 2016, **7**, 5526–5535.

18 (a) F. Suriano, O. Coulembier, J. L. Hedrick and P. Dubois, *Polym. Chem.*, 2011, **2**, 528–533; (b) M. Helou, O. Miserque, J.-M. Brusson, J.-F. Carpentier and S. M. Guillaume, *Chem. – Eur. J.*, 2010, **16**, 13805–13813; (c) A. P. Dove, *ACS Macro Lett.*, 2012, **1**, 1409–1412; (d) N. E. Kamber, W. Jeong, R. M. Waymouth, R. C. Pratt, B. G. G. Lohmeijer and J. L. Hedrick, *Chem. Rev.*, 2007, **107**, 5813–5840; (e) M. K. Kiesewetter, E. J. Shin, J. L. Hedrick and R. M. Waymouth, *Macromolecules*, 2010, **43**, 2093–2107; (f) L. Mespouille, O. Coulembier, M. Kawalec, A. P. Dove and P. Dubois, *Prog. Polym. Sci.*, 2014, **39**, 1144–1164.

19 P. Brignou, M. Priebe Gil, O. Casagrande, J.-F. Carpentier and S. M. Guillaume, *Macromolecules*, 2010, **43**, 8007–8017.

20 (a) S. Venkataraman, J. P. K. Tan, V. W. L. Ng, E. W. P. Tan, J. L. Hedrick and Y. Y. Yang, *Biomacromolecules*, 2017, **18**, 178–188; (b) S. Venkataraman, V. W. L. Ng, D. J. Coady, H. W. Horn, G. O. Jones, T. S. Fung, H. Sardon, R. M. Waymouth, J. L. Hedrick and Y. Y. Yang, *J. Am. Chem. Soc.*, 2015, **137**, 13851–13860.

21 A. K. Diallo, E. Kirillov, M. Slawinski, J.-M. Brusson, S. M. Guillaume and J.-F. Carpentier, *Polym. Chem.*, 2015, **6**, 1961–1971.

22 (a) F. D. Bobbink, W. Gruszka, M. Hulla, S. Das and P. J. Dyson, *Chem. Commun.*, 2016, 10787–10790; (b) M. Honda, M. Tamura, K. Nakao, K. Suzuki, Y. Nakagawa and K. Tomishige, *ACS Catal.*, 2014, 1893–1896; (c) G. L. Gregory, M. Ulmann and A. Buchard, *RSC Adv.*, 2015, **5**, 39404–39408.

23 J. A. Stewart, R. Drexel, B. Arstad, E. Reubsaet, B. M. Weckhuysen and P. C. A. Bruijnincx, *Green Chem.*, 2016, **18**, 1605–1618.

24 G. L. Gregory, L. M. Jenisch, B. Charles, G. Kociok-Köhn and A. Buchard, *Macromolecules*, 2016, **49**, 7165–7169.

25 K. Mikami, A. T. Lonnecker, T. P. Gustafson, N. F. Zinnel, P. J. Pai, D. H. Russell and K. L. Wooley, *J. Am. Chem. Soc.*, 2013, **135**, 6826–6829.

26 Y. Shen, X. Chen and R. A. Gross, *Macromolecules*, 1999, **32**, 2799–2802.

27 (a) O. Haba, H. Tomizuka and T. Endo, *Macromolecules*, 2005, **38**, 3562–3563; (b) M. Azechi, K. Matsumoto and T. Endo, *J. Polym. Sci., Part A: Polym. Chem.*, 2013, **51**, 1651–1655.

28 K. Tezuka, K. Koda, H. Katagiri and O. Haba, *Polym. Bull.*, 2015, **72**, 615–626.

29 (*a*) J. R. Tittensor and P. Mellish, *Carbohydr. Res.*, 1972, **25**, 531–534; (*b*) M. Suzuki, T. Sekido, S.-I. Matsuoka and K. Takagi, *Biomacromolecules*, 2011, **12**, 1449–1459.

30 G. L. Gregory, E. M. Hierons, G. Kociok-Köhn, R. Sharma and A. Buchard, *Polym. Chem.*, 2017, **8**, 1714–1721.

31 K. Fukushima, *Biomater. Sci.*, 2016, **4**, 9–24.

32 M. Pastusiak, P. Dobrzynski, J. Kasperczyk, A. Smola and H. Janeczek, *J. Appl. Polym. Sci.*, 2013, 40037.

33 (*a*) C. Fliedel, S. Mameri, S. Dagorne and T. Avilés, *Appl. Organomet. Chem.*, 2014, **28**, 504–511; (*b*) K. Kobayashi, S. Kanmuri, Y. Kimura and K. Masutani, *Polym. Int.*, 2015, **64**, 641–646.

34 P. Dobrzynski and J. Kasperczyk, *J. Polym. Sci., Part A: Polym. Chem.*, 2006, **44**, 98–114.

35 A. Couffin, D. Delcroix, B. Martín-Vaca, D. Bourissou and C. Navarro, *Macromolecules*, 2013, **46**, 4354–4360.

36 Y. Shen, X. Chen and R. A. Gross, *Macromolecules*, 1999, **32**, 3891–3897.

37 F. Nederberg, B. G. G. Lohmeijer, F. Leibfarth, R. C. Pratt, J. Choi, A. P. Dove, R. M. Waymouth and J. L. Hedrick, *Biomacromolecules*, 2007, **8**, 153–160.

38 O. Coulembier, V. Lemaur, T. Josse, A. Minoia, J. Cornil and P. Dubois, *Chem. Sci.*, 2012, **3**, 723–726.

39 M. Fineman and S. D. Ross, *J. Polym. Sci., Part A: Polym. Chem.*, 1950, **5**, 259–262.

40 D. J. Darensbourg, W.-C. Chung and S. J. Wilson, *ACS Catal.*, 2013, **3**, 3050–3057.

41 M. J. Frisch, G. W. Frucks, H. B. Schlegel, G. E. Scuseria, M. A. Robb, J. R. Cheeseman, G. Scalmani, V. Barone, B. Mennucci, G. A. Petersson, H. Nakatsuji, M. Caricato, X. Li, H. P. Hratchian, A. F. Izmaylov, J. Bloino, G. Zheng, J. L. Sonnenberg, M. Hada, M. Ehara, K. Toyota, R. Fukuda, J. Hasegawa, M. Ishida, T. Nakajima, Y. Honda, O. Kitao, H. Nakai, T. Vreven, K. Throssell, J. A. Montgomery, Jr., J. E. Peralta, F. Ogliaro, M. Bearpark, J. J. Heyd, E. Brothers, K. N. Kudin, V. N. Staroverov, R. Kobayashi, J. Normand, K. Raghavachari, A. Rendell, J. C. Burant, S. S. Iyengar, J. Tomasi, M. Cossi, N. Rega, J. M. Millam, M. Klene, J. E. Knox, J. B. Cross, V. Bakken, C. Adamo, J. Jaramillo, R. Gomperts, R. E. Stratmann, O. Yazyev, A. J. Austin, R. Cammi, C. Pomelli, J. W. Ochterski, R. L. Martin, K. Morokuma, V. G. Zakrzewski, G. A. Voth, P. Salvador, J. J. Dannenberg, S. Dapprich, A. D. Daniels, Ö. Farkas, J. B. Foresman, J. V. Ortiz, J. Cioslowski and D. J. Fox, *Gaussian 09, Revision D.01*, Gaussian, Inc., Wallingford CT, 2009.

42 (*a*) J.-D. Chai and M. Head-Gordon, *Phys. Chem. Chem. Phys.*, 2008, **10**, 6615–6620; (*b*) J.-D. Chai and M. Head-Gordon, *J. Chem. Phys.*, 2008, **128**, 084106.

43 M. Cossi, N. Rega, G. Scalmani and V. Barone, *J. Comput. Chem.*, 2003, **24**, 669–681.

44 J. Mindemark and T. Bowden, *Polymer*, 2011, **52**, 5716–5722.

45 E. Larsen, T. Kofoed and E. B. Pedersen, *Synthesis*, 1995, 1121–1125.

46 A. R. Vaino and W. A. Szarek, *Chem. Commun.*, 1996, 2351–2352.